

# A new approach to the solar oxygen abundance problem

R. Centeno

*High Altitude Observatory, NCAR, 3080 Center Green Dr, Boulder, CO 80301, USA*

rce@ucar.edu

H. Socas-Navarro

*High Altitude Observatory, NCAR<sup>1</sup>, 3080 Center Green Dr, Boulder, CO 80301, USA*

*Instituto de Astrofísica de Canarias, Avda Vía Láctea S/N, La Laguna 38205, Tenerife, Spain*

navarro@ucar.edu

## ABSTRACT

In this work we present new data that sets strong constraints on the solar oxygen abundance. Our approach, based on the analysis of spectro-polarimetric observations, is almost model-independent and therefore extremely robust. The asymmetry of the Stokes  $V$  profile of the 6300 Å [O I] and Ni I blend is used as an indicator of the relative abundances of these two elements. The peculiar shape of the profile requires a value of  $\epsilon_{\text{O}}=730\pm 100$  ppm (parts per million), or  $\log\epsilon_{\text{O}}=8.86\pm 0.07$  in the logarithmic scale commonly used in Astrophysics. The uncertainty range includes the model dependence as well as uncertainties in the oscillator strengths of the lines. We emphasize that the very low degree of model dependence in our analysis makes it very reliable compared to traditional determinations.

*Subject headings:* Sun: abundances – Sun: magnetic fields – Sun: atmosphere – techniques: polarimetric – line: profiles

---

<sup>1</sup>The National Center for Atmospheric Research (NCAR) is sponsored by the National Science Foundation.

## 1. Introduction

Oxygen is the third most abundant chemical element in the Universe, after Hydrogen and Helium, and the one that is almost exclusively produced by nuclear fusion in stellar interiors. Its abundance in the Sun was thought to be well established since the 1980s ( $\epsilon_{\text{O}}=850\pm 80$  parts per million, relative to hydrogen, ppm; Anders & Grevesse 1989; more recently  $\epsilon_{\text{O}}=680\pm 100$  Grevesse & Sauval 1998)<sup>1</sup>. However, a recent work (Asplund et al. 2004) using a new 3D hydrodynamical model of the solar atmosphere (as well as updated atomic and molecular data) recommends a revision of the O abundance to a lower value of  $\epsilon_{\text{O}}=457\pm 50$  ppm ( $\log\epsilon_{\text{O}}=8.66 \pm 0.05$ ). The revised solar composition is said to fit better within its galactic environment but it also creates a serious problem, namely it ruins the exceptionally good agreement between various predictions of solar interior models and properties inferred from helioseismology (see, e.g., Basu & Antia 2008).

The chemical composition of celestial bodies is not a directly measurable quantity. It is deduced by fitting observations with synthetic spectral profiles using a particular model atmosphere (temperature, density and so forth are prescribed), which makes it a strongly model-dependent process. Thus, the observations that lead to the O abundance are not conclusive and arguments exist both in favor and against the revision. The controversy on whether the proposed revision should be adopted and the doubts that it would cast on stellar structure and evolution models is serious enough that it is often referred to as the solar oxygen crisis (Ayres et al. 2006).

Both the traditional and the proposed revision of the O abundance have been obtained with similar sets of observations (an irradiance spectrum and an average disk center spectrum) and very similar techniques (fitting the equivalent width of atomic and molecular abundance indicators with synthetic spectra). The main difference prompting the revision is the model atmosphere employed for the synthesis. The traditional abundance is obtained when a semi-empirical one-dimensional (1D) model is used (e.g., that of Holweger & Mueller 1974), whereas the new low abundance is obtained when using a three-dimensional (3D) hydrodynamical simulation of photospheric convection (Asplund et al. 1999).

One criticism that has been formulated (Ayres et al. 2006) concerning the Asplund et al. (2004) work is that a 3D theoretical model is not necessarily superior to a 1D semi-empirical one when used to fit observations. This is a legitimate concern that deserves some consideration. An attempt to resolve the issue was made by Socas-Navarro & Norton (2007), who

---

<sup>1</sup> In this paper we use a linear abundance scale, given in ppm, because it is a more convenient unit in our approach. Some times, however, the traditional Astrophysical logarithmic scale is given to allow for easy comparison with previous work ( $\log\epsilon = 12 + \log_{10}[\epsilon \times 10^{-6}]$ ).

employed spatially-resolved observations of Fe I lines to derive a 3D semi-empirical model (thus combining the advantages of both strategies) and used it to analyze simultaneous spectra of the O I infrared triplet at 7770 Å. In this manner they derived  $\epsilon_{\text{O}}$  at each spatial position, as opposed to previous single-valued determinations, obtaining an average  $\epsilon_{\text{O}}=426$  ppm. While this result supports the new low abundance, the authors also pointed out that the spatial distribution of  $\epsilon_{\text{O}}$  exhibits an unsettling degree of structure, suggesting that the model is still less than perfect. This is not entirely surprising since the O I infrared triplet is strongly affected by non-LTE effects and it is possible that the line formation physics is not yet completely well understood.

In this work we take a novel approach and analyze Stokes  $V$  spectral data of the forbidden [O I] 6300 Å line. Its formation physics is much simpler than that of the infrared triplet, although it is a very weak line and is blended with a Ni I line of similar strength. This blend, rather than being a problem, turned out to be beneficial for our study because, even though it complicates the determination of  $\epsilon_{\text{O}}$ , it provides us with a nearly model-independent value of the ratio of  $\epsilon_{\text{O}}/\epsilon_{\text{Ni}}$  as we show below.

## 2. Data analysis and results

The observations employed here were acquired with the Spectro-Polarimeter for Infrared and Optical Regions (SPINOR, Socas-Navarro et al. 2006) on July 28, 2007. We obtained simultaneous observations of the Fe I lines at 6301.5 and 6302.5 Å and the 6300.3 Å blend of the [O I] and Ni I lines. The goal of our campaign was to observe a sunspot umbra because the different Zeeman splitting of the lines would allow us to differentiate them in the polarized spectrum. Since the Stokes  $V$  profile is normally antisymmetric, the spectral blend gives rise to a complex structure that provides us with important clues as we explain below. These lines are very weak and therefore it is important to observe a strongly magnetized region (ideally a sunspot umbra) to maximize the polarization signal. Besides, umbral profiles are very symmetric as velocity gradients are almost nonexistent in the umbral photosphere (below 100  $\text{ms}^{-1}$ ). Therefore, we can be certain that any asymmetries we may encounter are due to the presence of the blend.

We observed a small sunspot (solar activity was very low during our observing run) with moderate seeing conditions that we estimated to be approximately 1.5". Data reduction and polarization calibration were carried out using the standard procedures for this instrument, which include correction for the instrumental polarization introduced by the telescope. We selected the best datasets of July 28: two consecutive scans 20 minutes apart early in the morning, which we averaged; and a third scan taken later in the day. We shall refer to these

three datasets as Maps 1, 2 and 3, respectively.

Figure 1 shows the average Stokes  $V$  observed in the umbra of Map 1. All three datasets have a very similar average umbral profile. Also depicted in the figure are synthetic line shapes of the O (blue) and Ni (green) components of the blend computed separately as well as combined (red). The model atmosphere used for the synthesis was obtained from the inversion of the Fe I lines. All syntheses and inversions presented in this paper were carried out with the LTE code LILIA (Socas-Navarro 2001). Tests were conducted with another standard code (SIR, Ruiz Cobo & del Toro Iniesta 1992) using several of the models, to ensure that the same results were obtained.

Notice in Figure 1 how the [O I] and Ni I lines have similar amplitudes. However, the differences in their rest wavelengths and effective Landé factors give rise to a peculiar and strongly asymmetric shape of the blend when they are combined. Particularly interesting is the feature marked by the arrow in the figure, exactly at the switchover point between the [O I] and the Ni I blue lobes. This feature is present in all three of our datasets.

Consider the average of the slope of the red curve in the shaded area (hereafter referred to as  $m_{6300}$ ). If we had much more O than Ni, the red curve would follow the blue curve and this slope would be positive. Conversely, if we had much more Ni than O it would be the green curve that dominates and the slope would be negative. In an intermediate situation,  $m_{6300}$  takes values between these two limits. Figure 2 shows this behavior in detail for a range of the ratio  $\epsilon_{\text{O}}/\epsilon_{\text{Ni}}$  from low to high values. The amplitude of the profile and the vertical position of the central feature depend on the details of the model employed in the synthesis as well as the polarization calibration. However, the shape of the feature in the shaded area of Fig 2 (and therefore the mean slope  $m_{6300}$ ) is nearly model-independent, as we show below, which makes this feature valuable from a diagnostic point of view.

Table 1 lists the atomic parameters that we employed. Accurate determinations of the oscillator strength exist for all lines (Frose-Fischer & Saha 1983, Johansson et al. 2003, Bard et al. 1991; see also the database of the National Institute of Standards and Technology, NIST<sup>2</sup>), except for Fe I 6302.5 Å. We determined the  $\log(gf)$  of this line using the following procedure. We first inverted a spatially-averaged quiet-Sun profile of Fe I 6301.5 Å. With the resulting model we synthesized 6302.5 Å varying its  $\log(gf)$  until a satisfactory agreement with the observed profile was attained. We note that the accuracy of the Fe I oscillator strengths is not very important in our work. We use the Fe I lines to determine a suitable model atmosphere. However, the arguments given below are nearly model-independent. In fact, one could use standard sunspot models published in the literature and still obtain the

---

<sup>2</sup><http://physics.nist.gov/PhysRefData/ASD/index.html>

same results as we demonstrate using the model of Maltby et al. (1986).

The electric dipole and the magnetic quadrupole components of the [O I] feature are listed separately in the table, although the electric dipole contribution is insignificant. The two Ni I components correspond to the two major isotopes ( $^{58}\text{Ni}$  and  $^{60}\text{Ni}$ ): the relative abundances have been folded into the cited gf-values. The O I line is well described in LS coupling but the Ni I line exhibits some small departures (see the atomic level information compilation by NIST). We took this small departure into consideration in computing the polarized line profile.

We computed many different models by inverting the Fe I lines observed in the umbra of Maps 1, 2 and 3 (the profiles for Maps 1 and 2 were averaged together to improve the signal-to-noise ratio since they were taken very close in time) and using different values for the Fe abundance between 20 and 40 ppm. For each one of these models we synthesized the Stokes  $V$  spectrum (an example is shown in Fig 1) and computed  $m_{6300}$  as the average slope over a bandpass of 50 mÅ around the [O I] line center (the vertical shaded area in Fig 1). When performing all of these syntheses we added random perturbations to the oscillator strengths of the lines. The amplitude of these perturbations was set to the uncertainties in the values published in the literature (14% and 16% for the Ni I and O I lines, respectively). In this manner we could test the impact of these uncertainties on our results. The last column in Table 1 lists the range of abundances for the various elements involved in the synthesis that was used to produce the figure.

Figure 3 (blue shaded areas) shows how  $m_{6300}$  varies as a function of the O/Ni abundance ratio ( $\epsilon_{\text{O}}/\epsilon_{\text{Ni}}$ ). Note that all of these models produce a similar curve of  $m_{6300}$  vs  $\epsilon_{\text{O}}/\epsilon_{\text{Ni}}$ , regardless of which dataset we used to derive the model, what Fe abundance we considered, etc. The spread, delimited by the shaded region, is due a small degree of model dependence as well as the random variations in the O and Ni oscillator strengths. As a further test, we repeated the computation using a standard model umbra (model M of Maltby et al. 1986). The model temperature was first normalized to produce the observed continuum intensity (otherwise the ratio of O I to Ni I would be incorrect). The values of  $m_{6300}$  produced with the Maltby et al. (1986) model are still inside the band that we obtained with the models from our inversions. We may then conclude that the calibration curve of Fig 3 is extremely robust, in the sense that it exhibits very little sensitivity to the model atmosphere employed to obtain it.

The horizontal dashed line in Fig 3 marks the value  $m_{6300}$  of the observed profiles (along with the uncertainty due to observational noise), compatible with a ratio  $\epsilon_{\text{O}}/\epsilon_{\text{Ni}}=210\pm 24$ . Interestingly, the Ni abundance currently is better determined than that of O because there are more well-suited photospheric lines of Ni in the solar spectrum. Grevesse et al. (2007)

quote a current value of  $\epsilon_{\text{Ni}}=1.7\pm 0.15$  ppm, in good agreement with the meteoritic abundance of  $\epsilon_{\text{Ni}}=1.5\pm 0.1$ .

The abundance of *atomic* O that we obtain is  $\epsilon_{\text{O}}=360\pm 50$  ppm.

Since we are observing a sunspot, one must also be aware that some of the O may be in the form of molecules. Such molecular O does not contribute to the formation of the 6300 Å blend and has been neglected thus far. According to Lee et al. (1981), the most abundant O molecule (and the only one with a non-negligible concentration) in sunspot umbrae is CO, which contains nearly 50% of all the O. Instead of relying on this value, we made a full calculation for the temperature of our sunspot. We felt that this was important because, as noted above, the sunspot that we observed was a small one and it might be too warm compared to standard models. Our code solves the molecular chemical equilibrium for an arbitrary number of molecules. The interested reader can find a detailed account of the molecular calculation in a forthcoming research note. Here we shall simply state that 35 diatomic molecules which potentially can affect the atomic O and Ni partial pressures were included (Sauval & Tatum (1984)). The 6300 Å blend forms nearly at the same height as the continuum and therefore it is straightforward to obtain the temperature there. One simply needs to take the continuum intensity and equate it to the Planck function at that wavelength (as a sanity check, our inversions of the Fe I lines yield approximately the same temperature at  $\tau_{5000} = 1$ ). With this calculation we obtained that all the molecules containing O and Ni can be neglected except for CO, which carries about 51% of the O nuclei at that temperature.

It is important to note that the molecular calculation that we have solved is simply that of chemical equilibrium in LTE (no radiative transfer or spectral synthesis). The LTE/CE approximation is valid owing to the high densities of the umbral deep photosphere. This calculation does not require a model. Only the gas temperature is needed, which can be extracted directly from the observations as explained above. Therefore, we are not introducing any significant complication to our analysis. Putting all these numbers together we conclude that the total amount of O in the umbra is  $\epsilon_{\text{O}}=730\pm 100$  ppm, or  $\log\epsilon_{\text{O}}=8.86\pm 0.07$ .

### 3. Conclusions

Oxygen is a very important element because of its high abundance and also because other relevant elements that do not produce suitable photospheric lines can only be measured relative to it. Unfortunately, there are few O abundance indicators in the solar spectrum and they all present complications of one kind or another and require very detailed modeling to fit the observations. This means that virtually every abundance determination is susceptible

of criticism. Moreover, it is important to keep in mind that abundance determinations inherently are model-dependent.

In this work we present a new approach that circumvents these problems because: (a) we use a spectral feature whose formation physics is well known (LTE line formation, well-known oscillator strengths); and (b) the relation between the parameter  $m_{6300}$  and the ratio  $\epsilon_{\text{O}}/\epsilon_{\text{Ni}}$  is almost model-independent. By analyzing a polarization profile we are insensitive to common systematic errors, such as flatfield uncertainties (polarization is a differential measurement). The polarization profile of the 6300 Å feature is very peculiar. Instead of analyzing properties such as the amplitude of the profile, its width or depth, etc, which are sensitive to details of the modeling, we can focus on its shape. Some features such as  $m_{6300}$  depend very critically on the O and Ni abundances. The fact that the simplest O abundance indicator (only LTE atomic line in the visible spectrum) is blended with another line of similar strength has been viewed historically by many researchers as a rather unfortunate coincidence. In the light of this new approach, however, one could now argue the opposite. The abundances of O and Ni in the solar photosphere are “just right” to produce the peculiar polarization feature marked by the arrow in Fig 1. If either the O or the Ni line had dominated over the other then we would have had no other option than fitting the profile amplitude or width, which again would have been a model-dependent determination and therefore subject to question.

The ratio  $\epsilon_{\text{O}}/\epsilon_{\text{Ni}}=210\pm 24$  that we obtain is a very robust result and this ratio, combined with the well-established Ni abundance and taking into account that 51% of the O is in the form of CO, turns out to be incompatible with the low O abundance proposed by Asplund et al. (2004).

The authors are very grateful to Dr Thomas Ayres for pointing out the issue of the CO formation that we had missed in our initial manuscript. Without his suggestion this paper would have presented very different results. Thanks are also due to the staff at the Sacramento Peak observatory (Sunspot, NM, USA) of the National Solar Observatory for their enthusiastic support of our observing campaign. Financial support by the Spanish Ministry of Education and Science through project AYA2007-63881 is gratefully acknowledged.

## REFERENCES

- Anders, E. & Grevesse, N. 1989, *Geochim. Cosmochim. Acta*, 53, 197
- Asplund, M., Grevesse, N., Sauval, A. J., Allende Prieto, C., & Kiselman, D. 2004, *A&A*, 417, 751

- Asplund, M., Nordlund, Å., Trampedach, R., & Stein, R. F. 1999, *A&A*, 346, L17
- Ayres, T. R., Plymate, C., & Keller, C. U. 2006, *ApJS*, 165, 618
- Bard, A., Kock, A., & Kock, M. 1991, *A&A*, 248, 315
- Basu, S. & Antia, H. M. 2008, *Physics Reports*, 457, 217
- Frose-Fischer, C. F. & Saha, H. P. 1983, *Phys. Rev. A*, 28, 3169
- Grevesse, N., Asplund, M., & Sauval, A. J. 2007, *Space Science Reviews*, 130, 105
- Grevesse, N. & Sauval, A. J. 1998, *Space Science Reviews*, 85, 161
- Holweger, H. & Mueller, E. A. 1974, *Solar Phys.*, 39, 19
- Johansson, S., Litzén, U., Lundberg, H., & Zhang, Z. 2003, *ApJ*, 584, L107
- Lee, H. M., Kim, D. W., Yun, H. S., Beebe, R., & Davis, R. 1981, *Journal of Korean Astronomical Society*, 14, 19
- Maltby, P., Avrett, E. H., Carlsson, M., Kjeldseth-Moe, O., Kurucz, R. L., & Loeser, R. 1986, *ApJ*, 306, 284
- Ruiz Cobo, B. & del Toro Iniesta, J. C. 1992, *ApJ*, 398, 375
- Sauval, A. J. & Tatum, J. B. 1984, *ApJS*, 56, 193
- Socas-Navarro, H. 2001, in *Astronomical Society of the Pacific Conference Series*, Vol. 236, *Advanced Solar Polarimetry – Theory, Observation, and Instrumentation*, ed. M. Sigwarth, 487–+
- Socas-Navarro, H., Elmore, D., Pietarila, A., Darnell, A., Lites, B. W., Tomczyk, S., & Hegwer, S. 2006, *Solar Phys.*, 235, 55
- Socas-Navarro, H. & Norton, A. A. 2007, *ApJ*, 660, L153



Table 1. Atomic parameters

Ion	Wavelength (Å)	Excitation potential (eV)	$\log(gf)$	Configuration (lower)	Configuration (upper)	Landé factor	Abundance range (ppm)
O I	6300.304	0	-9.776	$^3P_2$	$^1D_2$	1.25	200-630
O I	6300.304	0	-12.202	$^3P_2$	$^1D_2$	1.25	200-630
Ni I	6300.335	4.266	-2.250	$^3D_1$	$^3P_0$	0.51	1-3
Ni I	6300.355	4.266	-2.670	$^3D_1$	$^3P_0$	0.51	1-3
Fe I	6301.501	3.654	-0.718	$^5P_2$	$^5D_2$	1.67	20-40
Fe I	6302.492	3.686	-1.235	$^5P_1$	$^5D_0$	2.50	20-40

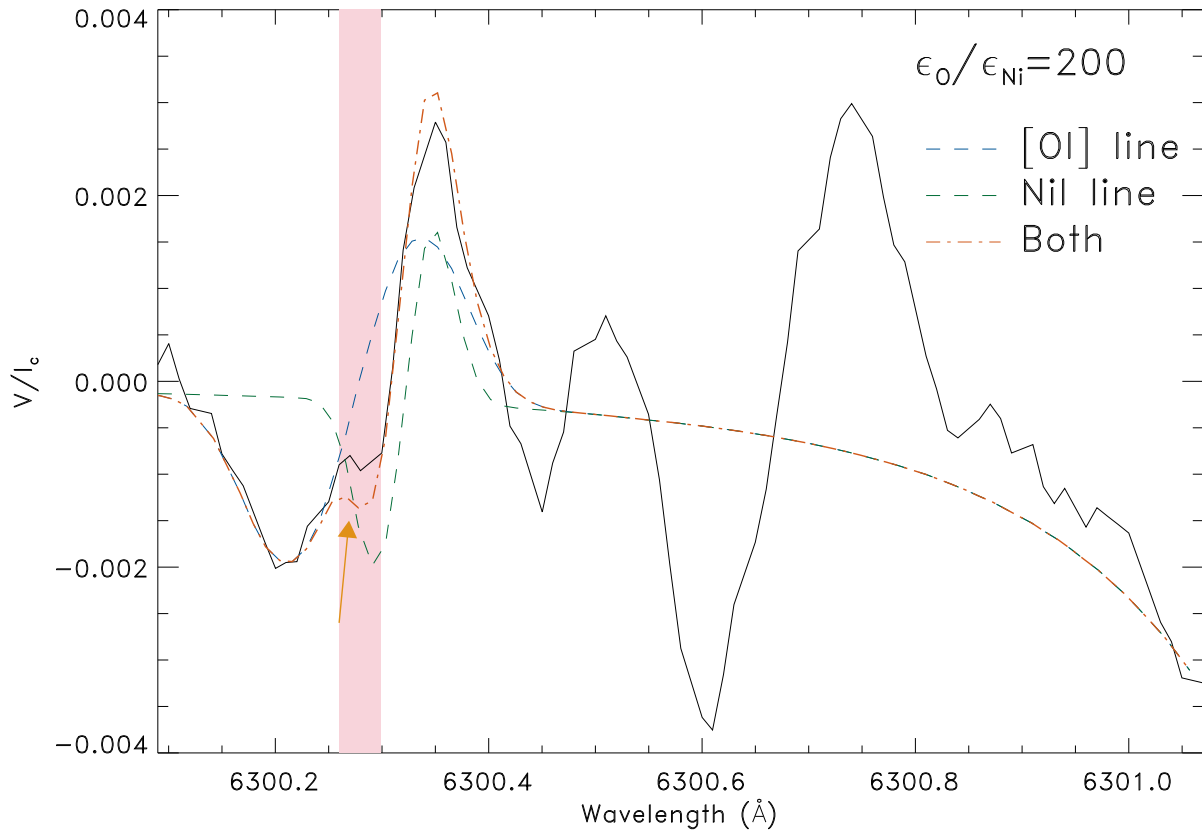


Fig. 1.— Stokes  $V$  spectrum of a sunspot umbra. Black, solid: observed. Red, dash-dotted: Synthesis of the [O I], Ni I and Fe I lines combined. Blue, dashed: Synthesis of [O I] and Fe I lines only. Green, dashed: Synthesis of Ni I and Fe I lines only. All profiles are normalized to the average disk-center quiet-Sun continuum.

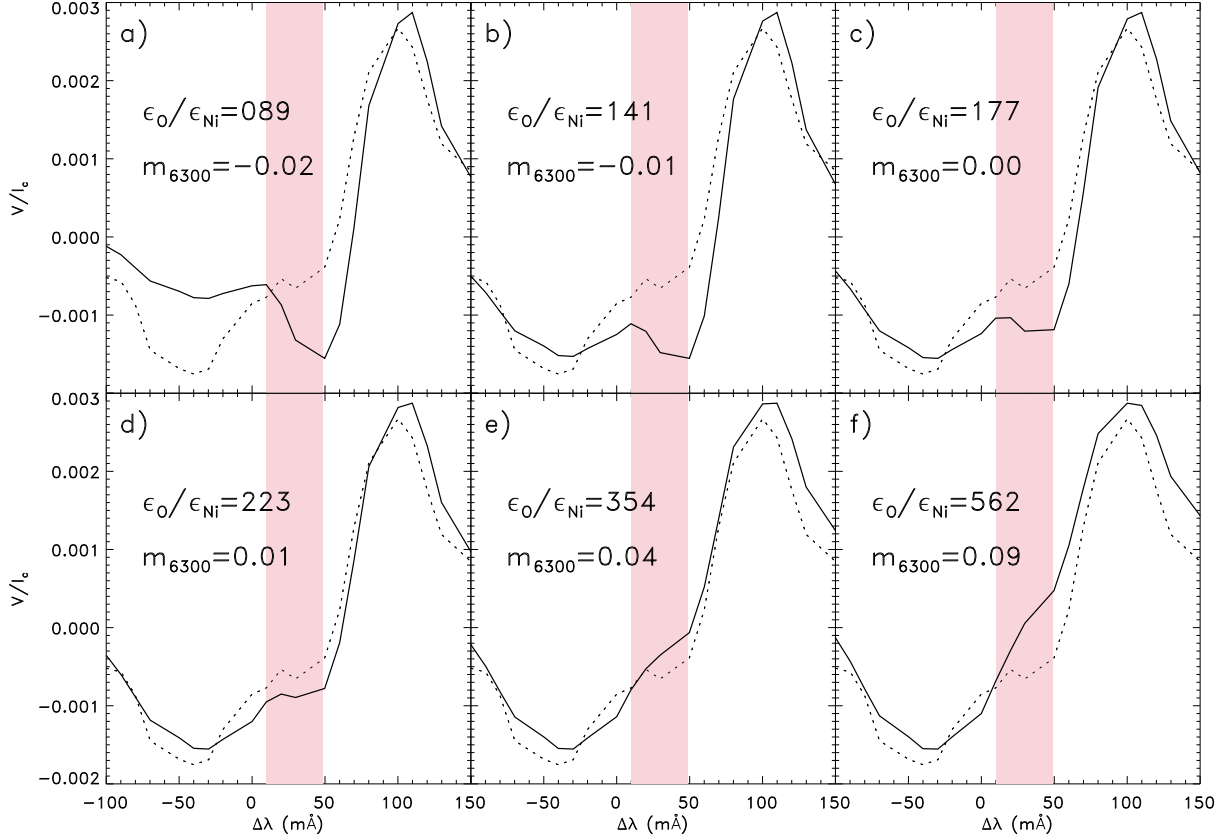


Fig. 2.— Synthetic Stokes  $V$  profile (solid) of the [O I]/Ni I blend for different values of the abundance ratio  $\epsilon_{\text{O}}/\epsilon_{\text{Ni}}$ . The shaded area represents the wavelength range over which we average the slope of the profile to obtain  $m_{6300}$ . For very low ratios (panel a), the slope is negative. As the ratio increases (panels b, c)  $m_{6300}$  becomes less negative until it reaches zero. For higher ratios  $m_{6300}$  continues to increase (panels d, e, f) until the [O I] line dominates the blend and the profile takes on the normal antisymmetric Stokes  $V$  shape of an isolated line. The profile amplitude and zero point depend on details of the model employed for the synthesis and the data calibration. For this reason, the profiles in the figure have been renormalized to have the same amplitude as the observed one (dotted line). However, the shape of the central feature in the shaded area and the mean slope  $m_{6300}$  are virtually model-independent. Therefore we base our analysis on this feature. After correcting for molecular formation, and assuming  $\epsilon_{\text{Ni}}=1.7$ , the ratios corresponding to the new and old O abundances would be 130 and 200, respectively. The corresponding profiles would be similar to those shown in panels b (new abundance) and d (old abundance).

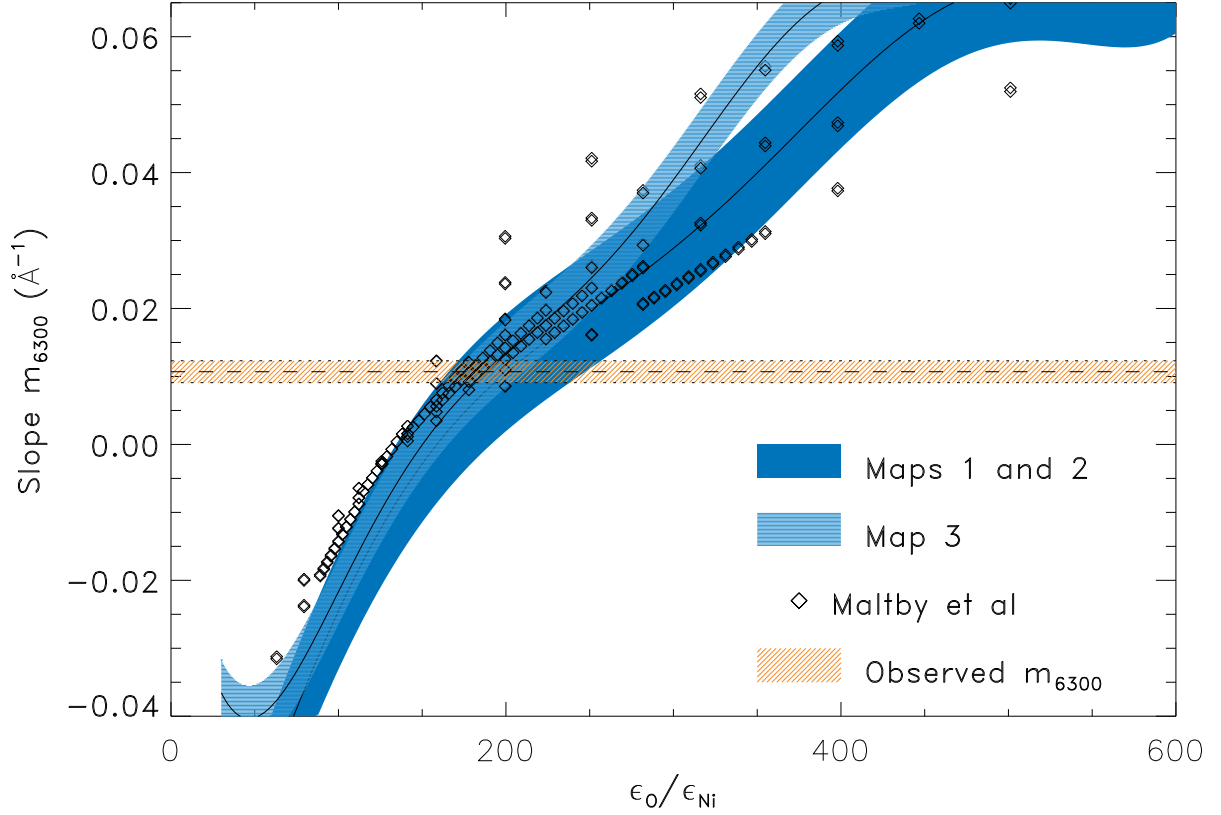


Fig. 3.— Mean slope  $m_{6300}$  of the central spectral feature (vertical shaded area in Fig 1) as a function of the abundance ratio between O and Ni ( $\epsilon_{\text{O}}/\epsilon_{\text{Ni}}$ ). The solid lines show the average curve obtained from many different inversions of the Fe I lines using different values for the Fe abundance, with  $\epsilon_{\text{Fe}}$  in the range 20, 40 ppm. The blue shaded areas represent the  $1\text{-}\sigma$  spread for all of those models. The diamonds represent the same curve obtained when a standard sunspot model (model M of Maltby et al. 1986) is employed. The horizontal dashed line shows the value for  $m_{6300}$  determined from the observed profile. The orange band indicates the uncertainty of the measurement due to noise. All three datasets yield a  $m_{6300}$  that is within the orange band.